FRONTISPIECE. The University of Michigan multispectral system uses double-ended optical mechanical scanners with various detector packages depending on the mission objectives. The configuration shown here was a 12-channel spectrometer on *End A* and a 3-element array on *End. B*.

DR. F. P. WEBER*
*USDA Forest Service*
*Berkeley, Calif. 94701*
F. C. POLCYN
*University of Michigan*
*Ann Arbor, Mich. 48107*

# Remote Sensing To Detect Stress in Forests

Availability of simultaneously registered data covering the entire bandwidth in narrow-band increments with optical-mechanical line scanners should yield improved accuracy.

*(Abstract on next page)*

## INTRODUCTION

A SUBSTANTIAL SUM is expended annually by government agencies and private organizations on surveillance and protection of forest resources in North America. The U. S. Forest Service, for example, spent more than 9 million dollars in 1969 in its detection

and suppression program nation-wide. A sizable portion of these dollars are used to find insect- and disease-infested trees.

Early detection of pest problem areas has received intensive research effort since the mid-1950's. Colwell's (1956) research was a catalyst for aerial photo investigations and particularly stimulated research with infrared films. Forest entomologists have successfully used, to some extent, both color and color infrared aerial photography for bark

163

beetle surveys (Ciesla 1967, Wert and Roettgering 1968, Heller and Wear 1969). These applications are limited, however, to locating infested trees after the foliage has visually faded.† The faded condition is frequently seen shortly before or often after adult beetle emergence; thus, some forest managers are understandably reluctant to use aerial methods as a detection tool for control purposes. French and Meyer (1969) report the successful use of color-infrared aerial photography for locating oak wilt-infected trees in central Minnesota. However, commission errors were high for the total disease-impact evaluation, particularly in trying to identify Dutch elm disease. *Fomes annosus* root rot has also been located on

differently from healthy vegetation in various portions of the electromagnetic spectrum. Polcyn *et al.* (1969) have reported on a multispectral sensing technique centered around the use of a simultaneous multichannel optical sensor. This sensor, developed at the University of Michigan, detected more of the information about an object's radiation than had been possible previously and permitted a new form of interpretation. It provided recording of energy levels in discrete bandwidths, yielding information not available to the human eye, and further, added the potential of automatic discrimination of objects from their unique spectral properties.

This paper reports a study to determine the usefulness of airborne multispectral remote

ABSTRACT: *The applications of airborne multispectral remote sensing and the potential of automatic multispectral processing offer a means for previsual detection of damage from insect infestations, disease organisms, and oxidant air pollution. Optical-mechanical line scanners flown over instrumented ground test sites in several different forest communities collected 18 discrete channels of remote sensing data between 0.4 and 13.5 micrometers. Reflective and emissive differences among stress-induced trees were well documented from ground measurements. The University of Michigan's multispectral optical-mechanical scanner and ground processing techniques were tested in terms of how they perform in detecting plant stress.*

aerial color infrared photographs in some instances (Murtha 1969).

Recent advances in aerial reconnaissance techniques, particularly in simultaneous recording of several spectral bands, seem to provide a potential previsual detection system. Work with agricultural crops has shown that differences exist between diseased and non-diseased and fertilized and unfertilized crops (Hoffer *et al.*, 1966) which permit separation of these conditions if the correct spectral bands are used. Similar techniques which permit detection of early physiologic disturbances in forest trees were reported by Weber (1969).

Wiegand *et al.* (1969) and others have reported on the reflective and emissive characteristics of agricultural vegetation under stress. That is, plants with abnormal biophysical response due to disruption of normal physiologic functions. Weber (1965) and Olson (1967) have reported the same information for forest trees. These studies have shown that vegetation under stress responds

† The term *faded* is a colloquial expression for a dying tree showing visible discoloration of foliage on aerial color photography.

sensing and automatic multispectral processing for previsual detection of damage to forests from insect infestations, disease organisms, and oxidant air pollution.

## FOREST PROTECTION PROBLEMS

The need to develop an efficient, reliable, previsual method of detecting forests under stress is shown by the huge losses from forest disturbances in the United States. The volume of timber lost annually often amounts to millions of board feet. The economic impact of losses from insects and diseases exceeds that of losses from fire by several times.

### BARK BEETLE DAMAGE

Recurrent losses from epidemics of the mountain pine beetle (*Dendroctonus ponderosae* Hopk.) in the central Rocky Mountain region have been observed before entomologists began recording attacks in this country. This insect is typical of a group of highly aggressive bark beetles which, like the southern pine beetle, can attack and kill thousands of vigorous, healthy pine trees during an epidemic.

Finding attacked trees has traditionally

been done by a combination of an aerial sketch-mapping technique (Heller *et al.* 1959) and an accurate ground sampling design (Knight 1958). More efficient methods are now needed because of the large expenditure of manpower and money needed to cover the large inaccessible land areas where infestations frequently occur. What is needed is a rapid method of detecting beetle-attacked trees over broad forested areas in advance of the visual symptoms that are presently required for an aerial photo technique. Bark beetle infestations, many with associated disease fungi, offer a special challenge for detection in remote forest areas, where outbreaks often surpass manageable levels before being reported.

ROOT ROT DAMAGE

Among forest diseases, *Poria weirii* root rot is especially destructive. It is responsible for extensive killing of 25- to 125-year-old Douglas-fir trees in the Pacific Northwest region of the United States. The disease is estimated to have an annual growth impact that exceeds 100 million cubic feet in the United States, but accurate figures are lacking because of inadequate detection and evaluation procedures.

Symptoms above the ground become evident only when the root rot has reached an advanced stage. External physical symptoms are characterized by foreshortened branch growth accompanied by a distressed crop of small cones. The next stage is a distinct thinning of foliage density. Unfortunately, these symptoms are not always in concert with a visible discoloration of the foliage. Frequently, the first indication an aerial observer has of the prevalence of *Poria weirii* in a forest stand is an opening in the crown canopy created by blowdown of weakened trees. All too often, however, infection centers have been discovered on the ground up to an acre in size with no blowdown. These centers cannot be detected on color or color-infrared aerial photography.

OXIDANT AIR POLLUTION DAMAGE

The third type of damage that might be identified by airborne multispectral remote sensing is air pollution damage to forest stands. This damage has manifested itself in many parts of the United States during the last two decades. In the East, coal-burning power plants were recognized early as a source of sulfur dioxide emissions shown to be very detrimental to the vigor of forest trees. More recently widespread damage to vegetation surrounding metropolitan centers from oxidant air pollution has been recognized. Extensive damage to high-value pine stands in the mountains surrounding the Los Angeles basin has been related to air pollution. A recent aerial survey of the Angeles National Forest, near Los Angeles, showed that 261,000 Jeffrey pine and Ponderosa pine suffered visible damage primarily from ozone in photochemical smog.* About 20 percent of those trees were severely affected and in an advanced condition of vigor decline.

A unique aerial survey method has been developed for assessing air pollution damage over large forest areas. It combines several scales of high-quality aerial color photography with multistage sampling theory (Wert 1969).

STRESS PARAMETERS IN FOREST TREES

Extensive ground instrumentation is frequently needed to establish stress parameters in forest trees and also to provide ground truth for airborne multispectral data. We have conducted basic studies on three National Forests representing different forest habitats to answer questions about changes in tree physiology and biophysical responses of stressed trees in relation to seasonal and diurnal changes in environment. The most direct benefit to the interpretation of airborne multispectral data has come from the energy budget studies. Although our data show the strong relationship between return energy characteristics measured just above the crown canopy and direct measures of tree vigor (e.g., rate of sap flow), it is the reflectance and emittance data which are most needed by image interpreters.

BARK BEETLE DAMAGE

Intensive studies were conducted for three years (1966 to 1968) on the Black Hills National Forest in South Dakota on the biophysical activity of bark beetle-infested trees. The primary objectives of the studies were: (a) to measure the biophysical activity of trees infested with the mountain pine beetle, and (b) to identify quantitatively (if possible) the sequential change in tree functions and activity from the time of initial beetle attack in August until the infested trees were dead the following summer. The continuous assessment of tree vigor in rela-

* Office report by Robert C. Heller, Project Leader, Remote Sensing Unit, Pacific Southwest Forest and Range Experiment Station, Berkeley, California, 1970.

tion to the environment was essential for understanding successes and failures in airborne detection. Because of the nature of beetle activity in the infested trees, and the associated destructive action of the blue stain fungi, most tree measurements and inferences had to do with water metabolism, leaf temperature, and energy exchange.

The bark beetle disturbance to ponderosa pine in the Black Hills is one of girdling the phloem and cambium cells, with some effect on the outer layers of xylem cells. This outer layer of xylem cells provides the most active pathway for translocation of water and mineral nutrients from the roots up the tree. The activity of the new beetle larvae, as a force of destruction to the pathway of water, begins in late summer or early fall. Weather condi-

tions during this initial period of larval feeding influence the rate of fading that will occur the following spring and summer. Although considerable penetration of blue stain and associated activity of beetle larvae have been observed in our study trees in fall, the most advanced condition of attack and infestation did not result in visual fading before winter (Figure 1). Reduced tree vigor in fall was shown through the effects on water translocation, transpiration, and to some extent, leaf temperature.

When physiologic activity in trees in the northern Black Hills will resume in spring is difficult to predict. Phenological development started by longer days and warmer temperatures vary widely from year to year. Although it progresses at much different rates between
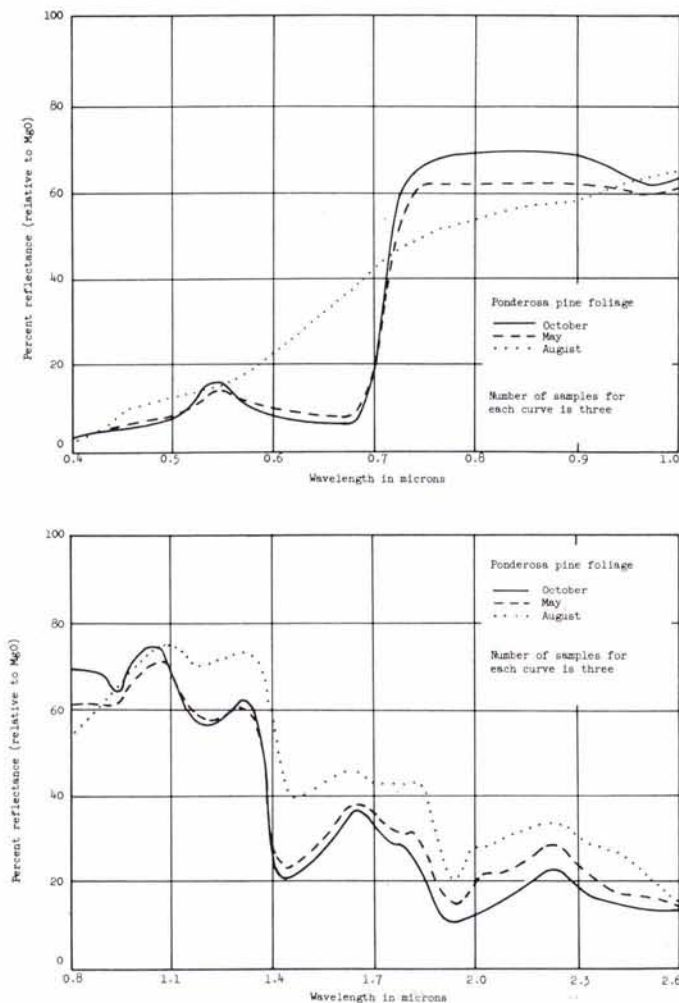


FIG. 1. Spectral reflectance curves of ponderosa pine show the effect of stress on reflectance 2, 9, and 12 months after attack by the mountain pine beetle in South Dakota.
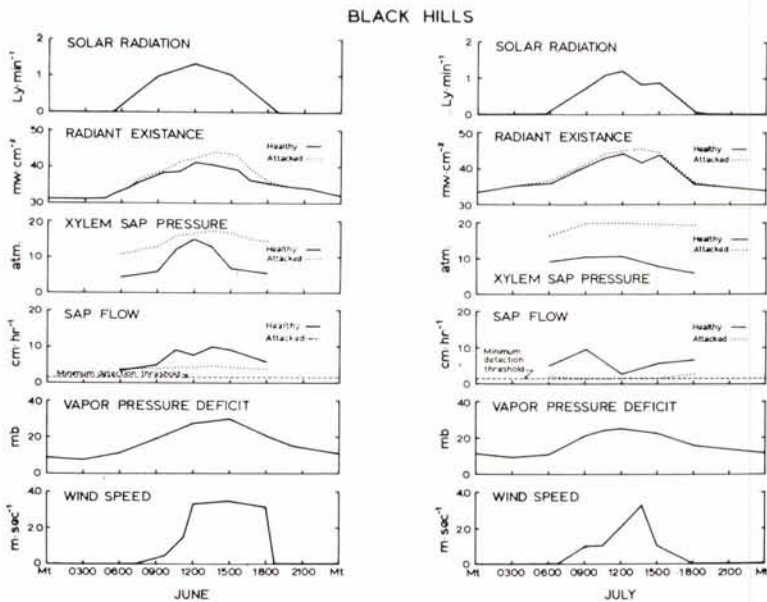
FIG. 2. Biophysical data recorded in South Dakota in June and July after beetle attack the previous August shows that greatest thermal radiance differences were measured in June.

April and June each spring, development does normalize by the first week in June (Figure 2). Therefore, it is important to monitor the critical indicator functions and energy exchange on the ground in order to insure any degree of success in aerial detection.

ROOT ROT DAMAGE

The apparent failure of aerial color and color-infrared photographs to reveal the location of *Poria weirii* root rot infection centers prompted us to consider the use of other remote sensing media. Some preliminary information on apparent temperatures of individual infected trees suggested that thermal infrared might be useful (Wear 1967).

In summer 1969 we began an intensive field study on the physiology and biophysical responses of second-growth Douglas-fir infected with root rot fungus on the Gifford Pinchot National Forest in Washington. A double tramway system was suspended between three 100-foot instrument towers to carry sensors for measuring the energy response from above both healthy and affected trees. The study site was selected next to the Wind River forest nursery in south central Washington. Scanning profiles of radiation data were recorded onto magnetic tape directly from the 38 sensors by way of a high-speed, analog-to-digital data logger. Biophysical data were recorded continuously in two separate modes: (1) at 1-second intervals while the tramways were moving, and (2) at 20-minute intervals while the trams were parked over benchmark trees (one healthy and one infected).

We found little in the thermal data to suggest there might be thermal radiance differences between tree condition classes. In fact, from intensive analysis of 120 continuous days of data, only isolated examples of thermal differences were found between healthy and infected trees. Those anomalous instances could not be related to any physiological or environmental phenomenon, although the latter is more likely to be true. We strongly believe that, ordinarily, thermal radiance differences between healthy and stressed trees are brought about through differential water availability and metabolism in the upper crown of large trees. In the case of *Poria weirii*, we could not measure consistent patterns of water use as a function of apparent tree condition.

The possibility of an important implication to remote sensing was derived from short-wave radiation data; that is, the 2 percent higher albedo at midday which was consistently recorded over infected trees as compared to healthy trees. Together with our other energy data this finding suggests that if a difference is to be detected by remote sensors, it will be between 0.7 and 1.8 $\mu$m.

OXIDANT AIR POLLUTION DAMAGE

To date, little has been done on the bio-physical instrumentation of high-stress trees suffering air oxidant injury. We have ana-lyzed a large number of spectral reflectance curves of needle samples taken from ponder-osa pine in three different vigor categories on the San Bernardino National Forest in southern California. The reflectance curves from samples taken in May suggest that the largest difference between vigor classes are in the 0.55 to 0.70 $\mu$m spectral band. However, these curves provide no information on thermal infrared differences beyond 2.6 $\mu$m.

Apparent temperature measurements were recorded over 29 trees with a portable radiom-eter in October 1969. Measurements were made in a three-day period by using a cherry-picker to place the radiometer and observer above the study trees. The data show a nar-row spread of the means of apparent temper-atures calculated for each tree condition class, with considerable overlapping of tempera-tures between classes.

Although the data provide only one sample in terms of seasonal changes, they do suggest the problems in thermal discrimination. Perhaps the biggest problem is the inadequate tree condition class codes based at present exclusively on external morphological fea-tures.

MULTISPECTRAL SYSTEM

The University of Michigan's multispec-tral system was developed in the early 1960's by the Infrared and Optics Laboratory, Willow Run Laboratories of the University's Institute of Science and Technology. It con-sisted of two double-ended optical-mechanical scanners which permitted placement of de-tector packages in four separate places. A key addition to the system was a prototype spectrometer which was mated to one of the two conventional optical-mechanical scan-ners. The basic configuration of the system has remained substantially the same, but en-gineering refinements were made when neces-sary.

CHARACTERISTICS AND CAPABILITY

Automatic registration is provided in both time and position with the 12-channel spec-trometer between 0.4 and 1.0 $\mu$m. This pro-vides simultaneous sensing in each wave-length band for each resolution element. The size of the resolution element at 1,000 ft alti-tude is 3×3 ft. In a second position a three-element detector array is individually filtered

to provide data in the 1.0–1.4 $\mu$m, 2.0–2.6 $\mu$m, and 4.5–5.5 $\mu$m or as the combination 1.0–1.4 $\mu$m, 1.5–1.8 $\mu$m, and 2.0–2.6 $\mu$m. In the last positions, a UV detector filtered be-tween .32–.38 $\mu$m or a Hg:Cd:Te detector filtered for 8–14 $\mu$m is normally employed.

The detector array where both near-IR and thermal-IR (4.5–5.5 $\mu$m) could be brought into simultaneity by electronic time delays was found to be particularly useful for de-tecting moisture stress as both a temperature rise and a reflectance change were expected from laboratory and field measurements.

The rotating element of the scanner has four flat surfaces at 45° from the rotational axis (Frontispiece). The collected energy is focused onto the detectors by a parabolic mirror. An image is generated by scanning perpendicular to the flight line and matching aircraft speed and scanner rotation speed to provide a contiguous image line by line. The scan synchronization and video data are stabilized about the roll axis of the airplane to reduce distortion. Data from all channels are tape-recorded. Another important feature is the use of reference plates and lamps as well as incorporating a sun reference signal. Each detector observing energy between 0.3 and 2.6 $\mu$m sequentially scans, (a) the scene below the aircraft, (b) two quartz-iodine reference lamps, and (c) a sky reference source which is mounted in the top of the aircraft in order to integrate the sky illumination. The zero reflectance level is provided by scanning the dark interior of the scanner housing.

For wavelengths longer than 2.6 $\mu$m, two blackbody plates, controllable over a tem-perature range of 0°C to 60°C, are used as reference sources for the infrared channels. Each plate is controlled (automatically heated or cooled as required to a set tempera-ture). One plate is set to a temperature near the lower range of interest in the scene and the second plate is set at a higher temperature over which the objects of interest may be found. These references have proven espe-cially useful in subsequent electronic slicingic procedures where quantitative temperature contours can be extracted. The use of the two blackbody plates limits the field of view of the second scanner system to 37 degrees in contrast to the first scanner (operating in the visible region) that records 80 degrees of the scene scanned.

DATA PROCESSING

Because the data from several channels are recorded on 14-channel magnetic tape in

registry and are referenced, a number of analog and digital processing techniques are available for processing the data.

Processing experiments were conducted at Willow Run Laboratories (WRL) with a special Spectral Analysis and Recognition Computer (SPARC). Two separate operations are performed on the SPARC. The first consists of selecting a training sample from the data (that is, some known point or area in the test scene) and storing the spectral characteristics (up to 12 channels of that area in the computer). The next operation then consists of recognizing all points in the scene which are statistically similar within a predefined criteria to the spectrum from the training set. A strip map is prepared wherein all points with similar spectral properties are printed as an enhanced image. Details of the mathematics for the decision criteria are given in Lowe, *et al.*, 1966.

By using a training set for each object of interest, the process can be repeated and each recognition map can be color-coded to display in one format the distribution of several objects. As the area of each resolution element is known, an area count of each set of objects is available immediately at the end of each run of data. And because the tape can be played back immediately, data can be analyzed without any delay on the computer.

So far, reliable spectral signatures can be obtained on objects whose size is approximately 4 or 5 resolution elements. At 1,000 ft altitude with 3 milliradians (mr) of system resolution, this capability means elements of the scene about 15 ft across can reliably be extracted if spectral differences exist with reflectance differences greater than 1 percent.

The statistical decision criteria and recognition processing can also be performed with digital techniques. A computer program has been developed to obtain the optimum set of 6 channels (from the 12 in the spectrometer) for best probability of detection and lowest false detection rate. Furthermore, preprocessing programs are available that make it easier to remove unwanted variations in the data due to angle effects (Malila 1968), shadows, and possible scanner nonuniform response over the total field of view so as to increase accuracy of recognition over the entire image of line flown. But if digital techniques are used alone, the speed of processing would be about 100 times slower.

Specialized single-channel processing is available and is used with the thermal 8–14 $\mu$m channel to produce a set of voltage slices corresponding to different temperature intervals. Inasmuch as the data are originally stored on magnetic tape, the electronic slicing is performed easily and more accurately than if the object is photographed and subsequently scanned with a densitometer over the gray tones of the film. Digital over-sampling of each resolution element of the analog tape is expected to produce the most accurate differentiation of small temperature differences.

In the past, the selection and weighting of spectrometer channels for visible and near-infrared data were often done in somewhat less than a scientific procedure. A more scientific approach is now possible through a recent development at WRL. We can now select the optimum spectrometer channels for a classification problem on a digital computer. A computer program called STEPER computes the average probability of misclassification for each pair of signatures which is the average probability of misclassifying signature 2 as signature 1 (Nalepka 1970). Then it adds the average probabilities of misclassification, weighting each entry with a specified weight. The result is an average pairwise probability of misclassification (APPM), with the best channel chosen as that channel with the lowest APPM.

We tested the optimum channel selection technique on three classification problems: the first, a generalized forest type classification; the second, classifying three conditions of tree vigor in ponderosa pine; and third, identifying nonfaded bark beetle-attacked ponderosa pine.

## RESULTS AND DISCUSSION

The ordering of the spectrometer channels in the first problem, for which all signatures were given equal weight, is shown in Table 1.

At each step, the channels for which the average pairwise probability of misclassification is computed includes all those channels previously selected plus the most recent addition to the set. Thus, by examining the affect of adding additional channels, it is possible to select the level of accuracy beyond which the addition of more channels adds little to accuracy.

The second problem was a classification of healthy, faded beetle-attacked, and old-killed ponderosa pine. In this problem all categories were given equal weight so that the channel choice would be equally influenced by the misclassification of one object as any other. The results agree with SPARC orderings calculated in the past for channel optimization (Table 2).

The 0.8 to 1.0 $\mu$m channel, which was first

TABLE 1. SPECTROMETER CHANNELS IN THE
ORDER SELECTED FOR CLASSIFICATION
OF FOREST TYPES

| Channel Number | Spectral Band | APPM* |
|---|---|---|
| 10 | 0.80–1.00 μm | 0.1676 |
| 8 | 0.66–0.72 μm | 0.1197 |
| 1 | 0.40–0.44 μm | 0.0930 |
| 6 | 0.58–0.62 μm | 0.0714 |
| 2 | 0.46–0.48 μm | 0.0613 |
| 9 | 0.72–0.80 μm | 0.0535 |
| 5 | 0.55–0.58 μm | 0.0471 |
| 3 | 0.50–0.52 μm | 0.0414 |
| 4 | 0.52–0.55 μm | 0.0360 |
| 7 | 0.62–0.66 μm | 0.0313 |

* Average pairwise probability of misclassification.

TABLE 3. SPECTROMETER CHANNELS IN THE ORDER
SELECTED FOR PROBLEMS IN CLASSIFYING
NONFADED, GREEN BEETLE-ATTACKED
PONDEROSA PINES

| Channel Number | Spectral Band | APPM* |
|---|---|---|
| 8 | 0.66–0.72 μm | 0.4304 |
| 3 | 0.50–0.52 μm | 0.3823 |
| 4 | 0.52–0.55 μm | 0.3273 |
| 7 | 0.62–0.66 μm | 0.2621 |
| 5 | 0.55–0.58 μm | 0.2297 |
| 6 | 0.58–0.62 μm | 0.1811 |
| 1 | 0.40–0.44 μm | 0.1570 |
| 9 | 0.72–0.80 μm | 0.1358 |
| 2 | 0.46–0.48 μm | 0.1187 |
| 10 | 0.80–1.00 μm | 0.1087 |

* Average pairwise probability of misclassification.

choice in the general classification, is last choice in the pine-type classification. The blue-violet channel was chosen as best and among the first six choices, two are in the red (channels 7 and 8), two in the green (channels 5 and 6), and two in the blue (channels 1 and 2).

The third and most difficult problem was the classification of healthy versus green beetle-attacked pine. In this instance only one pair of signatures existed. Compared with the classification of healthy, faded-attacked, and old-killed trees, the channel ordering was somewhat different (Table 3).

Among the best six channels for this problem were four of the best six channels for the second problem and only two of the best six channels for the general classification problem. Thus the choice of optimum channels for SPARC analysis for example is influenced by

TABLE 2. SPECTROMETER CHANNELS IN THE ORDER
SELECTED FOR PROBLEMS IN CLASSIFYING
VIGOR IN PONDEROSA PINES

| Channel Number | Spectral Band | APPM* |
|---|---|---|
| 1 | 0.40–0.44 μm | 0.3260 |
| 6 | 0.58–0.62 μm | 0.2636 |
| 5 | 0.55–0.58 μm | 0.2084 |
| 2 | 0.46–0.48 μm | 0.1820 |
| 7 | 0.62–0.66 μm | 0.1532 |
| 8 | 0.66–0.72 μm | 0.1292 |
| 9 | 0.72–0.80 μm | 0.1110 |
| 3 | 0.50–0.52 μm | 0.0957 |
| 4 | 0.52–0.55 μm | 0.0790 |
| 10 | 0.80–1.00 μm | 0.0700 |

* Average pairwise probability of misclassification.

the nature of the classification problem. We suggest that the digital channel optimization routine be used as the forerunner of a SPARC operation—especially if *a priori* knowledge is lacking for a classification problem.

Even if all 10 channels of data were used for classification, in this third problem there is still an APPM of about 10 percent between healthy and green attacked ponderosa pine. This is mediocre performance using all 10 available registered channels and attests to the difficulty of the problem in using visible and photographic (near-) infrared data.

Our past experience with SPARC processing has shown that many classification errors are made in identifying tree vigor if only visible and near IR channels were used. To see if any benefits accrued in using data representing a broader spectrum utilization of infrared radiance we combined reflective with thermal IR channels. Separate SPARC functions were performed on data collected over all three of our test sites (South Dakota, Washington, and California) with the multispectral system three-element IR array: 1.0–1.4 μm, 2.0–2.6 μm, and 4.5–5.5 μm (Figure 3).

Special considerations had to be taken into account for processing three-element data. In general spectral information from the scene point must be available in exact time-registration for analog processing on SPARC. The amount of tolerable delay is somewhat a function of target size (e.g., tree crown diameter). As we work with individual tree crowns in most applications, which tend to be small targets compared to the resolution element size, precise registration of data is required. Because the physical design of the three-element detector precludes precise registration, delay lines were wired into the SPARC
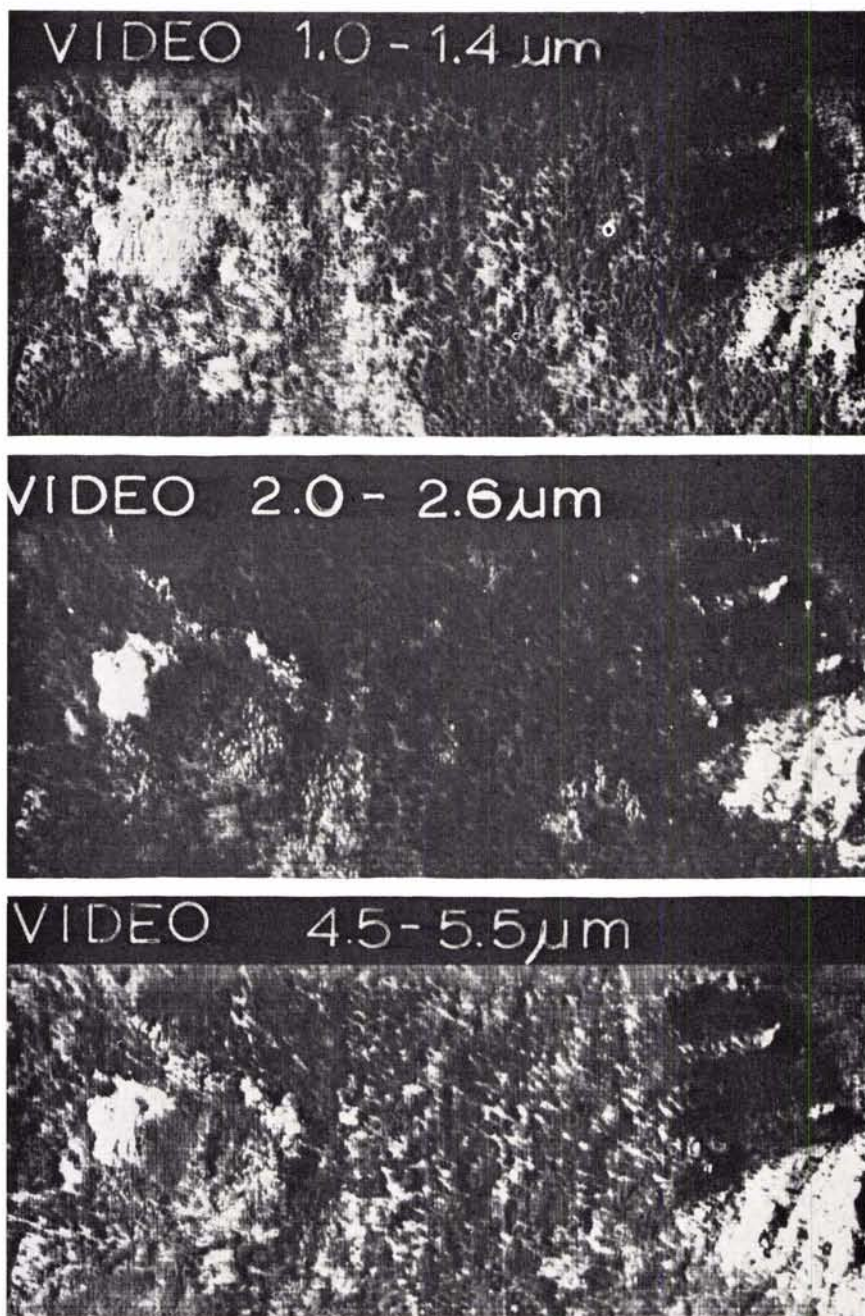
FIG. 3. Video imagery from the 3-element detector flown at 1,500 feet above the ground in the Black Hills illustrates the reflective infrared response from ponderosa pine forest. Note the high IR reflectance from the green and yellow/green beetle attacked trees on this early morning imagery. Most of the trees detected on the 2.0 to 2.6 μm imagery were not detected on 1:4,000 scale 70 mm color IR photos taken the same day.

logic to bring the analog signals from all three channels into exact registration.

The implementation of processing on SPARC consists of training and operations (Lowe, et al. 1966). In training, the spectral signatures of objects to be recognized are entered into SPARC which can generate the assumed Gaussian probability density functions. The

TABLE 4. THE 10-CHANNEL SPARC IDENTIFICA-
TION OF TREE CONDITION CLASSES BY EUCLIDEAN
DISTANCE ANALYSIS COMPARED WITH ACTUAL IN-
FESTATION GROUPS LOCATED IN THE FIELD

| Tree Condition | Actual Groups | SPARC Identifi- cation | Omission Errors | Commis- sion Errors |
|---|---|---|---|---|
| old-killed pine | 8 | 9[1] | 0 | 1 |
| faded attacked pine | 3 | 3 | 0 | 0 |
| nonfaded attacked pine | 6 | 11[2] | 1 | 6 |

[1] Includes one group of unfoliated hardwoods.
[2] Five actual infestation spots were identified along with six
erroneous spots which showed as two or more trees.

value of this function is a measure of how
closely a set of voltages from an area outside
the training set match the training-set volt-
ages. The voltages in each channel are propor-
tional to the spectral radiance in that channel.
Thus, the assumption in all processing is that
the spectral radiance of the object is charac-
teristic of that object. After the probability
density functions (PDF) were determined,
Euclidean distance processing was done by
printing out only those points where the PDF
was greater than an *a priori* threshold. Euclid-
ean distance analysis was quite successful
for 10-channel SPARC analysis (Table 4) but
was not sophisticated enough for the three-
channel IR data (Figure 4). We successfully
used maximum likelihood ratio analysis in
which the SPARC determines whether the
value of a likelihood ratio exceeds the thresh-
old value.

For the three-channel IR data from the
Black Hills test, training sets of hardwoods,
clearings, healthy pine, old-killed pine, and
green-attacked pine were made. The recogni-
tion map of hardwoods and clearings was
highly accurate. Similarly, the recognition of
old-killed pines was good, with only a few
false targets on the edges of the data. The
recognition of healthy pine was accurate ex-
cept in the immediate areas surrounding soil
and rock outcrops. The recognition of at-
tacked pines was lacking. In spite of prepro-
cessing, the spotty nature of recognition
seemed to be related to radiance variations
with topography for a given target.

For data from the Pinchot National Forest,
training sets were made up for alder, healthy,
fir, disease-infected fir, and two nursery areas
of different soil moisture. The recognition
map for alder and the two nursery types was
highly accurate with likelihood ratio process-
ing of the three-channel IR data. Healthy fir
was recognized adequately at the lower
threshold levels. Although a very tight model
for infected fir was developed on SPARC, likeli-
hood ratios and Euclidean distance process-

ing failed to identify infected trees outside
the training model. It seemed as though the
thermal data (4.5–5.5 µm) somehow con-
founded the model, whereas separation could
be attained by using only the two reflective
IR channels. Obviously this problem could be
solved with a single aperture spectrometer
having an extended range to 2.6 µm.

Extensive processing was done on our
southern California data using a seven-target
signature model which included conifer type
classification and three categories of vigor de-
cline in smog-affected ponderosa pine. Over-
all, the recognition techniques implemented
by SPARC processing fell short of producing an
accurate recognition map of affected pine
trees in three categories: severely affected,
moderately affected, and healthy. The princi-
pal problem was the large variation in the
signatures associated with vigor categories.
Also, no geometric continuity occurred with
regard to the distribution of trees belonging
to a particular category, so that the primary
target in each instance was an individual tree
crown of perhaps 10 to 20 feet in diameter.
Target size and continuity are not always a
consideration in multispectral processing,
but they are for most forestry applications.

Thermal infrared data collected over our
Black Hills test site in the 4.5–5.5 µm and the
8.2–13.5 µm wavelength bands were dis-
played as thermal contours created by a
thermal slicing technique. Each data slice
produced a data bit on negative film for ob-
jects of precisely the same apparent tempera-
ture. Meaningful slices were added together
and color-coded to produce a thermal con-
tour. The contouring steps were compared to
the original analog image and the target class
represented in any one step were identified
by using high-quality, large-scale aerial
color photography. All similar targets were
coded the same color and, when placed in a
color mosaic, permitted separation of classes
based on color code (Table 5).

Successful thermal separations were made
on the 8.2–13.5-µm imagery. Foliage on the
green-attacked pine was only a few degrees
warmer than the foliage of healthy trees.
This difference suggests that attacked trees
are thermally masked frequently by radiance
variations of healthy trees—a finding sub-
stantiated by ground data. For example, coni-
fers were separated on five contouring steps
with an apparent temperature spread of
3.5°C (Table 5).

A complication with the interpretation of
thermal responses in forests is that terrain
objects are detected on more than one con-
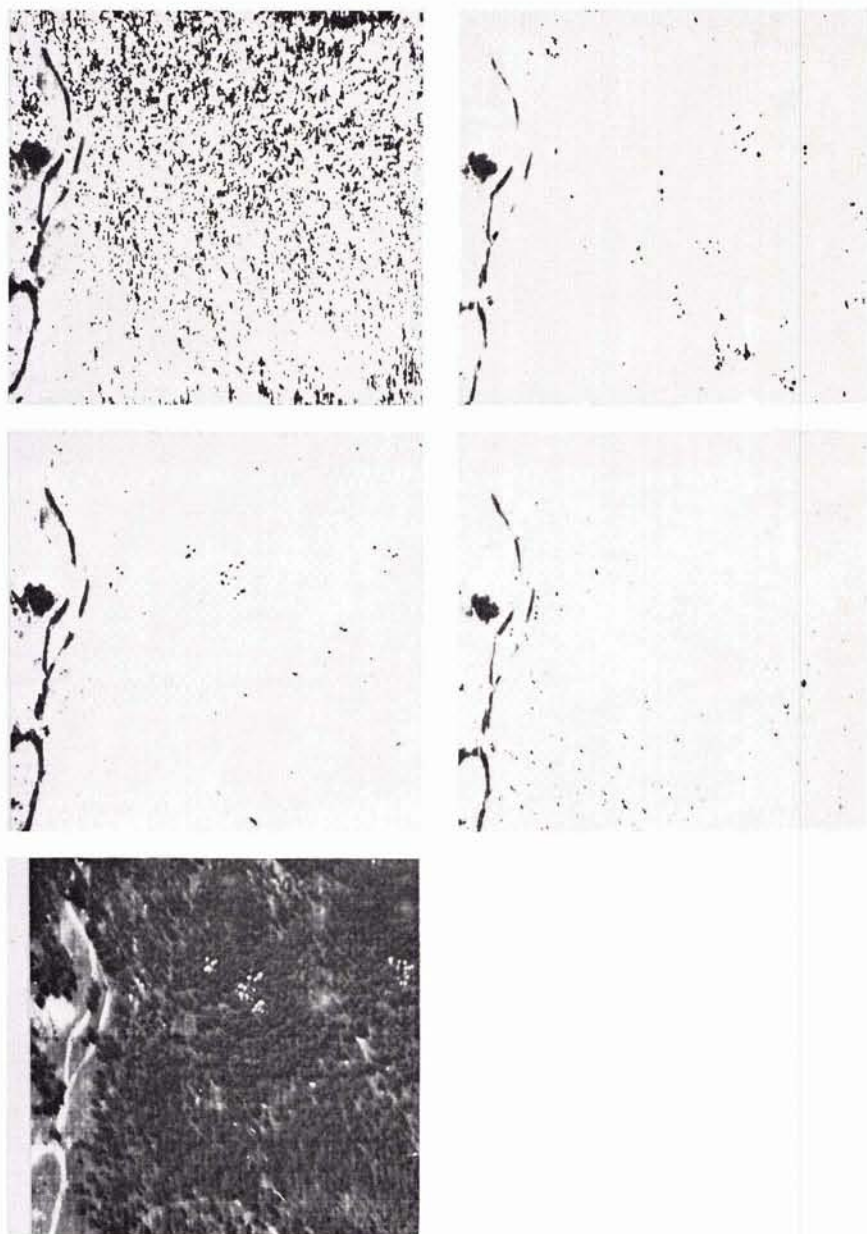touring step largely because of variations in

FIG. 4. Target recognitions resulting, from SPARC processing of 10-channel spectrometer data imaged over the Black Hills test site. Recognitions are as follows: *upper left,* healthy pine; *upper right,* old beetle killed pine; *center left,* faded beetle attacked pine; *center right,* non-faded (green) beetle attacked pine; and, *bottom left,* .62 to .66 µm video with recognition of faded attacked pine.

slope and target aspect. For example, conifers in the same condition class on different slopes are revealed in several different steps. This problem, due to different environmental thermal budgets, is further complicated if temperature variations occur over the size of a resolution element so that averaging takes place.

## Conclusions

For optimum detection of forest stress conditions it may be necessary to design and construct special scanner systems owing to the requirement of high spatial resolution to achieve a high sampling rate for small crown-diameter trees and conifer types as well as for large crown-diameter broadleaf

TABLE 5. DETAILED KEY TO THERMAL CONTOUR-
ING STEPS FOR IDENTIFICATION OF BLACK HILLS
TARGETS. DATA WAS COLLECTED WITH A 8.2 TO
13.5 MICROMETER DETECTOR FLOWN 5,000
FEET ABOVE THE GROUND AT 1325
HOURS ON JULY 22, 1969

| Step Number | Apparent Temp (K.) | Color Codes | Target |
|---|---|---|---|
| 10000 | 296.0 | yellow | grass |
| 10001 | 297.0 | dark green | hardwoods |
| 10011 | 297.5 | light blue | hardwoods with few conifers |
| 10101 | 298.0 | dark blue | conifers with few hardwoods |
| 10111 | 298.5 | magenta | conifers |
| 11000 | 299.5 | red | open grown and dead conifers |
| 10010 | 301.0 | brown | attacked conifers |
| 10110 | 304.0 | light green | exposed soil and grass |
| 10100 | 306.0 | olive | sparse grass and shrubs over bare soil |
| 01111 | 313.0 | orange | exposed rock and soil |

trees. This work would have to be done with-out sacrificing signal-to-noise ratio $(S/N)$ capability which relates to the minimum detectable differences in temperature.

As we see it, the greatest and most direct benefit to forest biologists from an improved multispectral system will be the previsual detection of stress in bark beetle-infested trees. We were able to show some detection success working independently with each of three spectral bandwidths ($0.4$–$1.0$ $\mu$m, $1.0$–$4.5$ $\mu$m, and $8.2$–$13.5$ $\mu$m). The availability of simultaneously registered data covering the entire bandwidth in narrow-band increments should yield large improvements in accuracy of stress detection. The benefits derived from a single-aperture system for identification of root rot infections and classification of air oxidant injury to conifers are less certain. Research is continuing to provide answers to these questions*.

## ACKNOWLEDGEMNTS

* Since this paper was written, the new Michigan M-7 scanner has been developed having simultaneously registered data covering the entire band width in narrow-band increments.

## REFERENCES

Ciesla, W. M., 1969. "Operational Use of Infrared Color Photography for Estimating Population Levels of Southern Pine Beetle Infestation," *Proceedings of the Workshop on Aerial Color Photography in the Plant Sciences*, University of Florida, Gainesville, Florida, 117–120.

Colwell, R. N., 1956. "Determining the Prevalence of Certain Cereal Crop Diseases by Means of Aerial Photography," *Hilgardia*, 26(5): 223–286.

French, D. W. and Meyer, M. P., 1969. "Aerial Survey for Oak Wilt and Dutch Elm Disease in Bloomington, Minnesota," *Proceedings of the Workshop on Aerial Color Photography in Plant Sciences*, University of Florida, Gainesville, Florida, 77–80.

Heller, R. C., Bean, J. L., and Knight, R. B., 1959, *Aerial Survey of Black Hills Beetle Infestations*. Forest Service, U. S. Department of Agriculture, Rocky Mountain Forest and Range Experiment Station, Paper 46.

Heller, R. C., and Wear, J. F., 1969. "Sampling Forest Insect Epidemics with Color Films," Proceedings of the Sixth Symposium, *Remote Sensing of Environment*, The University of Michigan, Ann Arbor, Michigan, 1157–1167.

Hoffer, R. M., Holmes, R. A., and Shay, J. R., 1966. "Vegetable, Soil, and Photographic Factors Affecting Tone in Agricultural Remote Multispectral Sensing," *Proceedings of the Fourth Symposium, Remote Sensing of Environment*, The University of Michigan, Ann Arbor, Michigan, 115–134.

Knight, F. B., 1958. "Methods of Surveying Infestation of the Black Hills Beetle in Ponderosa Pine," *Forest Science* 4(1): 35–41.

Lowe, D. S., Braithwaite, J. G. N., and Larrowe, V. L., 1966. "An Investigative Study of a Spectrum-Matching Imaging System," *Final Report* No. 8201-1-F, Willow Run Laboratories, Institute of Science and Technology, The University of Michigan, Ann Arbor, October 1965.

Malila, W., 1968. "Multispectral Techniques for Contrast Enhancement and Discrimination," *Photogrammetric Engineering*, 34(6), June 1968.

Murtha, P. A., 1969. "Optical Density Evaluation of *FOMES ANNOSUS* on False-Color Aerial Photographs," *Proceedings of the Workshop on Aerial Photography in the Plant Sciences*, University of Florida, Gainesville, Florida, 100–103.

Nalepka, R. F., 1970. "Investigation of Multispectral Discrimination Techniques," *Report No.* 2264-12-F, Willow Run Laboratories of the Institute of Science and Technology, The University of Michigan, Ann Arbor, Michigan.

Olson, C. E., Jr., 1967. "Optical Remote Sensing of the Moisture Content of Fine Forest Fuels," Unpublished report to the Forest Service, U. S. Department of Agriculture, Washington, D. C., by Willow Run Laboratories of the Institute of Science and Technology, The University of Michigan, Ann Arbor, Michigan.

Polcyn, F. C., Spansail, N. A., and Malila, W. A., 1969. "How Multispectral Sensing Can Help the Ecologist," In *Remote Sensing in Ecology*, University of Georgia Press, Athens, Georgia, P. L. Johnson (ed.), 194–218.

Wear, J. F., 1967. "The Development of Spectro-Signature Indicators of Root Disease on Large

Forest Areas," *Scientific and Technical Aerospace Reports*, NASA.

Weber, F. P., 1965. "Exploration of Changes in Reflected and Emitted Radiation Properties for Early Remote Detection of Tree Vigor Decline," Master's Thesis, The University of Michigan, Ann Arbor, Michigan.

Weber, F. P., 1969. "Remote Sensing Implications of Water Deficit and Energy Relationships for Ponderosa Pine Attacked by Bark Beetles and Associated Disease Organisms," Doctoral Dissertation, The University of Michigan, Ann Arbor, Michigan.

Wert, S. L., and Roettgering, B., 1968. "Douglas-Fir Beetle Survey with Color Photos," *Photogrammetric Engineering* 34(12):1243–1248.

Wert, S. L., 1969. "A System for Using Remote Sensing Techniques to Detect and Evaluate Air Pollution Effects on Forest Stands," *Proceedings of Sixth Symposium, Remote Sensing of Environment*, The University of Michigan, Ann Arbor, Michigan.

Wiegand, C. L., et al., 1969. "Spectral Survey of Irrigated Region Crops and Soils." *Scientific and Technical Aerospace Reports*, NASA.

# Theses and Dissertations

*Compiled by Lawrence W. Fritz*

*Devoted to achievements in graduate photogrammetric research*

PURDUE UNIVERSITY
SCHOOL OF CIVIL ENGINEERING
LAFAYETTE, INDIANA 47907

PH.D. DISSERTATIONS

*Ballew, R. W.*, "Planetary Gravitational Fields from Orbital Photogrammetry," June 1971.
*Collins, J.*, "Logarithmic Spirals for Computation of Distances on the Ellipsoid," August 1971.
*Kurtz, M. K. Jr.*, "Potential Uses of Holography in Photogrammetric Mapping," August 1971.